❒    317

# Nondestructive Determination of Beans Water Absorption Capacity using CFA Images Analysis for Hard-to-Cook Evaluation

**Ousman Boukar[a,b], Laurent Bitjoka[a,b], Gamraïkréo Djaowé[a,b]**
[a]Electrical Engineering and Industrial Automation Laboratory, Modelisation Image Processing and Applications Research Group, The University of Ngaoundere, Cameroon
[b]Biophysics and Food Biochemistry Laboratory, National School of Agro-Industrial Sciences, The University of Ngaoundere, PO Box 455 Ngaoundere, Cameroon

| Article Info | ABSTRACT |
|---|---|
| | Hard to cook (HTC) phenomenon is developed by storing bean grains under the adverse conditions of high temperature ($\geq 25$ °C ) and high humidity ($\geq 65$ %). Bean grains that have undergone this HTC phenomenon are characterized by loss of color lightness, development of browning and darkening, and decrease of Water Absorption Capacity (WAC). The objective of this study was to develop a CFA (Color Filter Array) image processing system to measure Water Absorption Capacity (WAC) of bean grains with high precision in short time intervals (10 min). The relationships between the CFA image features, extracted from raw images captured by CCD (charge coupled device) camera, and the measured WAC were established. The calibration models using multiple linear regression (MLR) were developed to predict WAC. The MLR models for prediction samples resulted in correlation coefficient ($R^2$) in the range of 0.811 to 0.947, standard error of prediction (SEP) in the range of 7.587 to 11.669, and Fisher variable value (F) in the range of 52.300 to 221.690. Results indicate that computer vision system (CVS) based on CFA image analysis technique can provide an accurate, reliable and nondestructive measurement method of WAC to evaluate the hard to cook defect in bean grains.<br><br> |

*Corresponding Author:*

Ousman Boukar,
The University of Ngaoundere, P.O. Box 455 Ngaoundere, Cameroon
Tel: +237 96 19 90 80; Fax: +237 22 15 81 89
E-mail address: boukarousman@gmail.com

## 1.    INTRODUCTION

Beans (Phaseolus vulgaris) are the third most important legume in the world on the basis of total grain production after soybeans and peanuts; they are a staple food in some tropical and subtropical countries [1]. Bean grains are a good source of carbohydrates and proteins. They provide important quantities of protein, starch, dietary fiber, protective phytochemicals, oil, vitamins and mineral elements [2]. Bean grains quality is determined by soaking characteristics, cooking and nutritive value [3]. Acceptability characteristics have not received enough attention in breeding programs. These traits include grain size, shape, color, appearance, stability under storage conditions, cooking properties, quality of the product obtained and flavor [1]. Despite the advantages that beans are a good food source, bean grains have some undesirable characteristics that limit their acceptability or nutritional value, such as: hard to cook (HTC) phenomenon, antinutriments or antinutritional factors or limitation in some amino acids of high biological value [4], [5], [6]. Hard to cook phenomenon is developed by storing bean grains under the adverse conditions of high temperature ($\geq 25$ °C ) and high humidity ($\geq 65$ %). This phenomenon is characterized by extended cooking

times for cotyledon softening [7]-[11]. Bean grains that have undergone this HTC phenomenon require increased energy (fuel) cost for preparation; are less acceptable to the consumer due to changes in flavor, color, and texture; and have decreased nutritive quality [12]. Several hypotheses have been proposed to explain the cause of bean grains hardening: lipid oxidation and/or polymerization, formation of insoluble pectates, lignification of middle lamella, and multiple mechanisms. Several methods have been proposed to study the hard to cook of bean, namely the determination of the cooking time [13]-[14], the determination of the water absorption capacity [8] and recently the determination of the cooking time-constant [15]. These methods are laborious, time consuming and invasive since they destroy the analyzed sample. Therefore, color and Water Absorption Capacity (WAC) might be related to each other. This has been proved by previous studies [16], in which color varied as WAC changed in bean grains during the storage at high temperature and high relative humidity. However, no clear relationship was established in these studies and any prediction models were not found to measure WAC as a function of color attributes. Therefore, the objective of this study was to develop an image processing system to measure WAC of beans with high precision in short time intervals (10 min). Images features of beans were obtained by computer vision while WAC was obtained by physico-chemical analysis.

The sensor is usually the most expensive component of the digital camera. To reduce cost and complexity, digital camera manufacturers often use a single CCD (charge coupled device) or CMOS (complementary metal-oxide semiconductor) sensor covered by a color filter array (CFA). The acquired image is a gray-scale image and thus, digital image processing solutions should be used to generate a camera output comparable to the one obtained using a three-sensor device. The acquired image is called CFA image. In order to analyze images in higher precision, rapidly with a low cost method, CFA images were used in this work.

This paper is divided in the following principal sections: section 2 describes the materials And methods, section 3 shows experimental results and discussion, and section 4 presents the the authors Conclusions.

## 2.    MATERIALS AND METHODS
### 2.1. Beans samples and hardening procedure
Bean (Phaseolus vulgaris) grain samples of five freshly harvested varieties, namely, DOR-701, MERINGUE, SENEGALAIS, ECAPAN-021 and MAC-55 were obtained from the Regional Center for Research and Innovation West, Bafoussam, Cameroon. The different varieties of bean grains samples used in this study are given in Table1. Hardened beans were produced using the accelerated storage procedure [16] Everyday, 40 bean grains were sampled and previously analyzed through algorithms developed using the computer vision system (CVS) before using them to measure the WAC.

Table 1. Bean samples used in this study.

| samples | varieties | Captured images |
|---|---|---|
| Red bean | DOR-701 | |
| Red bean | MERINGUE | |
| Speckled bean | ECAPAN-021 | |
| Speckled bean | MAC-55 | |
| Red bean | SENEGALAIS | |

## 2.2. Method of water absorption capacity (WAC) determination

WAC was determined using the Paredes-López et al. (1986) procedure with minor variations. Before analysis, samples were adjusted to the same moisture content (14%). 40 beans were selected. Whole seeds were soaked in two volumes of distilled water at 25 °C. After 24h of soaking samples were removed, drained, blotted and weighed. The increment in weight was reported as WAC per 100 g of dry weight and was calculated using the following formula:

$$WAC\left(\%\right) = 100 \ \frac{M_1\left(weightofso\ akedbeans\ \right) - M_0\left(weightofdr\ ybeans\ \right)}{M_0\left(weightofdr\ ybeans\ \right)} \tag{1}$$

## 2.3. CFA Images acquisition

CFA images were captured using an image acquisition system of a digital color camera similar to that developed by Bitjoka*et al*. (2010), and Mery and Pedreschi (2005) (Figure 1). This image acquisition system is a box type enclosure. Samples were illuminated by using four parallel fluorescent lamps with a color temperature of 6500 K (Philips, Natural Daylight, 40 W) and a color rendering index (Ra) near to 95%. The four lamps were situated 40 cm above the samples and at angle of 45° of the food sample plane. This illumination system gave a uniform light intensity over the food plane. A CCD digital color camera (FUJIFILM Finepix HS10), was located vertically at a distance of 25cm from the samples through a hole on the top surface of the box. The angle between the camera lens axis and the lighting sources was around 45°. Sample illuminators were inside a wood box whose internal walls were painted white, firstly to increase contrast and eliminate areas with grey levels close to white [17] and secondly to assure a uniform illumination inside the room [18]. Images were captured with the mentioned CCD digital color camera with its maximum resolution (3664 X 2742 pixels), and stored as a raw image without compression. The raw image stored was a CFA image and was denoted $I^{CFA}$. The white balance of the CCD digital color camera was set using a simple white reference. Color standards were photographed and analyzed periodically to ensure that the lighting system and the CCD digital color camera were working properly. The CFA images of beans were acquired everyday over a period of project to show different levels of hardening.
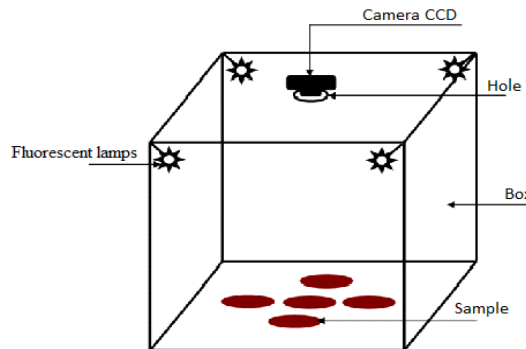


Figure 1. Schematic representation for bean grains image acquisition system

## 2.4. CFA Image pre-processing

Images captured by CCD digital color camera are subject to various types of noises. These noises may degrade the quality of an image and subsequently it cannot provide correct information for subsequent image processing. In order to improve the quality of an image, some operations need to be performed on it to remove or decrease degradations suffered by the image during its acquisition. The purpose of pre-processing is an improvement of the image data, which suppresses unwilling distortions or enhances some image features that are important for further processing and creates a more suitable image than the original for a specific application. Pre-processing method used in this study is similar to the one reported by Du and Sun (2004). Our local pre-processing method focus on acquiring CFA image of bean grains with a white scene content. The white scene content in the CFA image, denoted $L$, had equal responses in all color components ($R^{CFA,} = G^{CFA} = B^{CFA}$), with the midtones being rendered near the middle of the tone scale, regardless of the illuminant or content of the scene. Correction image adjustment was accomplished by multiplying pixels in each color component ($R^{CFA,}$, $G^{CFA}$ and $B^{CFA}$) by any different gain factor (a, b, c) which compensates for a

non-neutral CCD digital color camera response and illuminant imbalance. The corrected CFA image was denoted $\widetilde{I}^{CFA}$ . The corrected CFA image or the corrected pixels values were obtained as follows:

$$\begin{bmatrix} \widetilde{R}^{CFA} \\ \widetilde{G}^{CFA} \\ \widetilde{B}^{CFA} \end{bmatrix} = \begin{bmatrix} a & 0 & 0 \\ 0 & b & 0 \\ 0 & 0 & c \end{bmatrix} \begin{bmatrix} R^{CFA} \\ G^{CFA} \\ B^{CFA} \end{bmatrix} \tag{2}$$

$$\begin{cases} a = \dfrac{\overline{K}_0}{\overline{R}^L} \\[2ex] b = \dfrac{\overline{K}_0}{\overline{G}^L} \\[2ex] c = \dfrac{\overline{K}_0}{\overline{B}^L} \end{cases} \tag{3}$$

$$\begin{cases} \overline{R}^L = \dfrac{1}{Card\left(R^{CFA} \cap L\right)} \sum_{p \in R^{CFA} \cap L} I^{CFA}(p) \\[3ex] \overline{G}^L = \dfrac{1}{Card\left(G^{CFA} \cap L\right)} \sum_{p \in G^{CFA} \cap L} I^{CFA}(p) \\[3ex] \overline{B}^L = \dfrac{1}{Card\left(B^{CFA} \cap L\right)} \sum_{p \in B^{CFA} \cap L} I^{CFA}(p) \end{cases} \tag{4}$$

Where $I^{CFA} = \left[R^{CFA} + G^{CFA} + B^{CFA}\right]$, $\widetilde{I}^{CFA} = \left[\widetilde{R}^{CFA} + \widetilde{G}^{CFA} + \widetilde{B}^{CFA}\right]$, $I^{CFA}(p)$ is the level value of the pixel $p$, $\overline{K}_0$ isthe white reference value, and $\overline{R}^L$ , $\overline{G}^L$ and $\overline{B}^L$ correspond to the mean value of the pixels of $R^{CFA} \cap L$, $G^{CFA} \cap L$ and $B^{CFA} \cap L$ , respectively.

## 2.5. CFA image segmentation



(a)
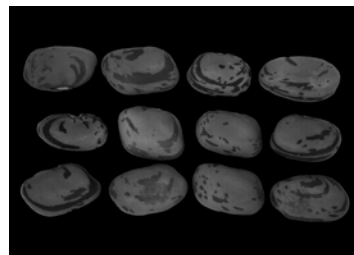


(b)

Figure 2. Segmentation procedure: (a)original CFA image and (b)segmented CFA image

Since the acquired images contained both the bean sample and background, a technique capable of removing the background from the images is a prerequisite for the color analysis procedures that follow. An algorithm for segmenting bean sample from the background was developed using ImageJ code. The developed segmentation algorithm was based on the Otsu thresholding method [19] to automatically calculate the optimum threshold value; the computing method of optimum threshold value was described in details by Chen and Qin (2008). Segmentation was performed using the following three steps; (i) separating bean sample from the background, (ii) removing of noise from the binary image, and (iii) filling of holes in the segmented binary image to obtain an actual binary image. The bean sample (or beans pixels) were denoted $H$ and the background $\overline{H}$. One image of the sample and the segmented result are illustrated in Figure 2.

## 2.6. CFA images features extraction

Features of the bean samples were extracted from $R$ (red), $G$ (green) and $B$ (blue) components of the CFA images. For each of the three color components, their mean and standard deviation values were calculated and, consequently, 6 CFA images features including three means values ($\mu^R$, $\mu^G$, $\mu^B$) and three standards deviations ($\sigma^R$, $\sigma^G$, $\sigma^B$) were obtained [20]. The means show the average color properties of bean grains and the standard deviations represent a measure of color un-uniformity over a bean grain. They were calculated by the following equations:

$$\mu^R = \frac{1}{Card\left(H \cap R^{CFA}\right)} \sum_{p \in H \cap R^{CFA}} \widetilde{I}^{CFA}(p) \tag{5}$$

$$\mu^G = \frac{1}{Card\left(H \cap G^{CFA}\right)} \sum_{p \in H \cap G^{CFA}} \widetilde{I}^{CFA}(p) \tag{6}$$

$$\mu^B = \frac{1}{Card\left(H \cap B^{CFA}\right)} \sum_{p \in H \cap B^{CFA}} \widetilde{I}^{CFA}(p) \tag{7}$$

$$\sigma^R = \sqrt{\frac{1}{Card\left(H \cap R^{CFA}\right)} \sum_{p \in H \cap R^{CFA}} \left[\widetilde{I}^{CFA}(p) - \mu^R\right]^2} \tag{8}$$

$$\sigma^G = \sqrt{\frac{1}{Card\left(H \cap G^{CFA}\right)} \sum_{p \in H \cap G^{CFA}} \left[\widetilde{I}^{CFA}(p) - \mu^G\right]^2} \tag{9}$$

$$\sigma^B = \sqrt{\frac{1}{Card\left(H \cap B^{CFA}\right)} \sum_{p \in H \cap B^{CFA}} \left[\widetilde{I}^{CFA}(p) - \mu^B\right]^2} \tag{10}$$

Where $\widetilde{I}^{CFA}(p)$ is the level value of the corrected pixel $p$.

## 2.7. Data analysis

To develop a prediction model of *WAC* of the bean grains using their extracted CFA image features, multiple linear regression (MLR) analysis was applied to build the model of prediction [21]-[22]. MLR analysis between WAC and CFA image features extracted was conducted using Statgraphics Plus for Windows software, Version 5.1 at 95% of confidence level. The aim of MLR analysis is to find a mathematical relationship between a set of independent variables, *X* matrix (14 storage days observation × 6 CFA image features), and the dependent variable, *Y* matrix (14 storage days observation × 1 *WAC*). The values of the attribute *WAC* of the calibration set were used to represent the dependent variable *Y*. Meanwhile, the 6 CFA image features of the bean samples represented the independents variables or the predictors (*X*). The linear equation between the 6 CFA image features ($\mu^R, \mu^G, \mu^B, \sigma^R, \sigma^G, \sigma^B$) and the Water Absorption Capacity (*WAC*), was defined as follows:

$$\hat{WAC} = b_0 + b_1\mu^R + b_2\mu^G + b_3\mu^B + b_4\sigma^R + b_5\sigma^G + b_6\sigma^B + \varepsilon \tag{11}$$

Where $\hat{WAC}$, predicted value of the attribute; $b_0$, $b_1$, $b_2$, $b_3$, $b_4$, $b_5$, $b_6$, regression coefficients of the equation to be estimated; and $\varepsilon$, the standard error between the predicted and measured values. Once the linear regression model was determined, the equations were used to predict the attributes of samples in the calibration and validation sets. The quality of the calibration model was evaluated by the standard error of calibration (*SEC*), standard error of prediction (*SEP*), the multiple correlation coefficient ($R^2$) between the predicted and measured value of the attribute [23]-[24], the Fisher variable value (*F*). A good model should have a low SEC, a low SEP, a high R, a small difference between SEC and SEP [21] and a high F. The predictive ability of the models were also quantified by these criteria. The results of future predictions with a 95% confidence interval can be expressed as the predicted value $WAC_i \pm 1.96 \times SEC$ [24]. These criteria are defined as follows:

$$SEC = \sqrt{\frac{1}{n_c}\sum_{i=1}^{n_c}\left(\hat{WAC_i} - WAC_i\right)^2} \tag{12}$$

$$SEP = \sqrt{\frac{1}{n_p}\sum_{i=1}^{n_p}\left(\hat{WAC_i} - WAC_i - bias\right)^2} \tag{13}$$

$$bias = \frac{1}{n_p}\sum_{i=1}^{n_p}\left(\hat{WAC_i} - WAC_i\right) \tag{14}$$

$$R^2 = \left(\frac{SEC}{SEO}\right)^2 \tag{15}$$

$$SEO = \sqrt{\frac{1}{n_c}\sum_{i=1}^{n_c}\left(\overline{WAC} - WAC_i\right)^2} \tag{16}$$

$$\overline{WAC} = \frac{1}{n_p}\sum_{i=1}^{n_c} WAC_i \tag{17}$$

$$F = \frac{n_c - k - 1}{k}\left(\frac{SEC}{SER}\right)^2 \tag{18}$$

$$SER^2 = SEO^2 - SEC^2 \tag{19}$$

Where, $\hat{WAC_i}$ represents the predicted value of the i-th observation; $WAC_i$ represents the measured value of the i-th observation; $n_c$ is the number of observations in calibration set; $n_p$ is the number of observations in prediction set; $k$ is thenumber of CFA image features.

## 3. RESULTS AND DISCUSSION
### 3.1. Water Absorption Capacity (WAC) determination
Figure 3 shows the effect of storage on *WAC* of the five bean grains varieties. In the fresh state, MERINGUE variety had higher *WAC* value than the other varieties. Accelerated storage caused a significant ($p < 0.05$) decrease in the *WAC* of the whole bean grain samples, being more pronounced in the MERINGUE variety. SENEGALAIS variety had lower decrease of *WAC* than the other varieties. The decrease in the *WAC* of the bean grains was reported by other authors [25], [26], [7]; these results showed that beans stored under tropical conditions absorb less water during soaking, which itself may contribute to a harder bean texture. The results obtained in the present study were in agreement with the results presented by Reyes-Moreno *et al.* (2000)*,* whichsuggested that changes of a biochemical and/or physico-chemical nature in both the cotyledon and seed coat result in a lower water uptake capacity.

The curves presented in Figure 3 show that a *WAC* constant was found for each bean variety. These *WAC* constants could characterize the age and the hardening of each bean grain variety and could be used to predict the maximum storage time of each bean variety under the tropical conditions; high temperature and high relative humidity. The *WAC* constants obtained were in the range of -0.198 to -0.113. This study suggests that higher is the absolute value of *WAC* constant, rapidly could be the hardening process of the bean grain. Furthermore, lower is the absolute value of *WAC* constant; slowest could be the hardening process of the bean grain.
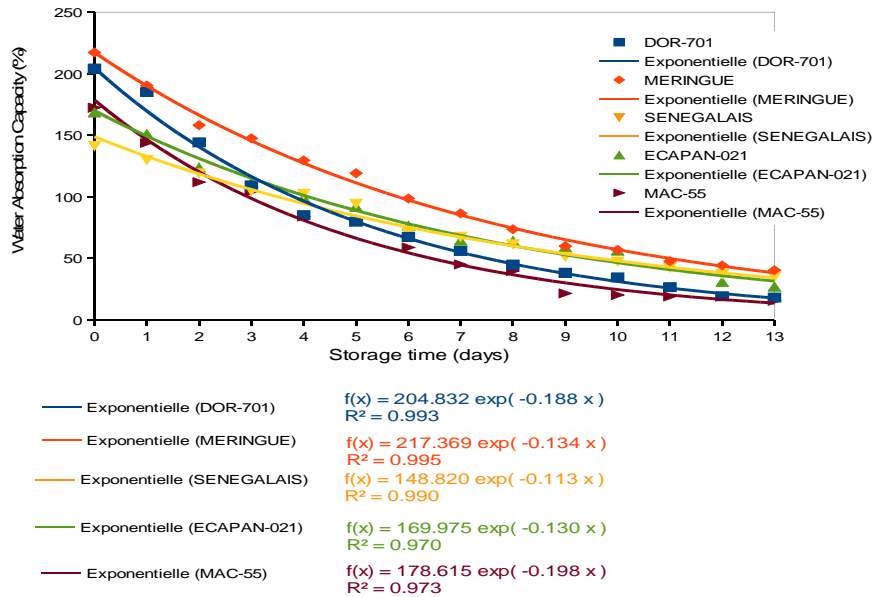


Figure 3. Relation between water Absorption capacity and storage time in the five varieties of common bean (Phaseolus vulgaris)

## 3.2. CFA image features extraction

Six features characterizing color of the bean grains were extracted from the CFA images of bean grains. The effect of storage on CFA image features of the five varieties is outlined in Figures 4a-e. In general, at all times and for the whole bean grain varieties, the $\mu^R$ value was ($p < 0.05$) higher than both the $\mu^G$ and $\mu^B$ values; except the MERINGUE variety where $\mu^R$ value was lower than both the $\mu^G$ and $\mu^B$ values after ninth storage day. Furthermore, the $\sigma^R$, $\sigma^G$, $\sigma^B$ values were ($p < 0.05$) similar for all times and for the whole bean grain varieties. Storage produced a significant ($p < 0.05$) decrease of the $\mu^R$, $\mu^G$ and $\mu^B$ values of the five bean varieties, however a significant ($p < 0.05$) decrease of the $\sigma^R$, $\sigma^G$, $\sigma^B$ values was obtained in the ECAPAN-012 and MAC-55 varieties. However, no significant ($p < 0.05$) decrease of the $\sigma^R$, $\sigma^G$, $\sigma^B$ values was obtained in the DOR-701, MERINGUE and SENEGALAIS varieties and could not be used also as a CFA image features indicators to establish *WAC* calibration models. The $\mu^R$, $\mu^G$, $\mu^B$, $\sigma^R$, $\sigma^G$ and $\sigma^B$ curves of the DOR-701, MERINGUE, SENEGALAIS, and ECAPAN-021 varieties presented an exponential effect, while the same features presented a logarithmic effect for the MAC-55 variety. Theses curves effects showed that the five studied varieties of beans were browned and darkened during the storage at high temperature and high humidity. Other researchers [27],[16],[1],[7]reported a similar behavior in common beans during storage at high temperature and high humidity. The results of this study suggest that a significant browning and darkening were developed at the bean grain surface during the storage at high temperature and high humidity, being more pronounced in red bean than speckled bean.
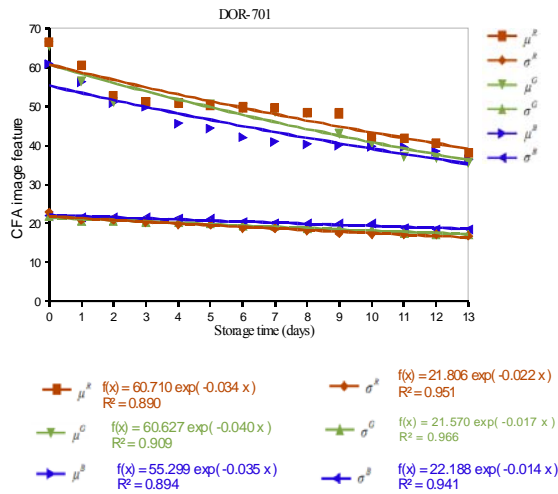
**DOR-701**

$\mu^R$
$\sigma^R$
$\mu^G$
$\sigma^G$
$\mu^B$
$\sigma^B$

CFA image feature — Storage time (days)

| | | | |
|---|---|---|---|
| $\mu^R$ | f(x) = 60.710 exp( -0.034 x) R² = 0.890 | $\sigma^R$ | f(x) = 21.806 exp( -0.022 x) R²=0.951 |
| $\mu^G$ | f(x) = 60.627 exp( -0.040 x) R² = 0.909 | $\sigma^G$ | f(x) = 21.570 exp( -0.017 x) R² = 0.966 |
| $\mu^B$ | f(x) = 55.299 exp( -0.035 x) R² = 0.894 | $\sigma^B$ | f(x) = 22.188 exp( -0.014 x) R² = 0.941 |

Figure 4a. Relation between 6 CFA image features and storage time in the DOR-701 variety

**MERINGUE**

$\mu^R$
$\sigma^R$
$\mu^G$
$\sigma^G$
$\mu^B$
$\sigma^B$

CFA image feature — Storage time (days)

| | | | |
|---|---|---|---|
| $\mu^R$ | f(x) = 76.679 exp( -0.060 x) R² = 0.935 | $\sigma^R$ | f(x) = 20.816 exp( -0.017 x) R² = 0.955 |
| $\mu^G$ | f(x) = 59.869 exp( -0.036 x) R² = 0.882 | $\sigma^G$ | f(x) = 21.595 exp( -0.017 x) R² = 0.927 |
| $\mu^B$ | f(x) = 62.061 exp( -0.030 x) R² = 0.844 | $\sigma^B$ | f(x) = 23.223 exp( -0.019 x) R² = 0.938 |
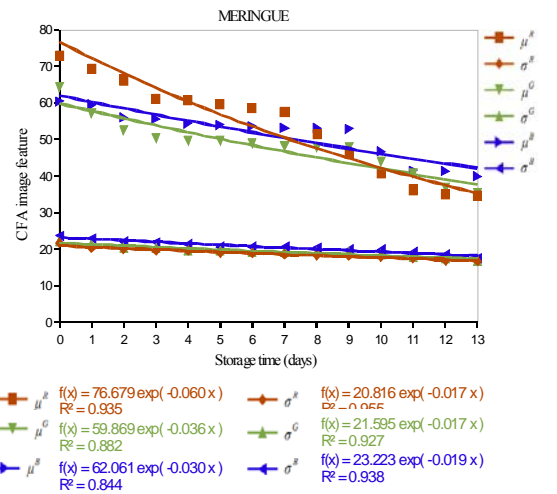
Figure 4b. Relation between 6 CFA image features and storage time in the MERINGUE variety

**SENEGALAIS**

$\mu^R$
$\sigma^R$
$\mu^G$
$\sigma^G$
$\mu^B$
$\sigma^B$

CFA image feature — Storage time (days)

| | | | |
|---|---|---|---|
| $\mu^R$ | f(x) = 86.754 exp( -0.074 x) R²=0.930 | $\sigma^R$ | f(x) = 19.198 exp( -0.019 x) R²=0.939 |
| $\mu^G$ | f(x) = 75.798 exp( -0.062 x) R²=0.970 | $\sigma^G$ | f(x) = 19.227 exp( -0.019 x) R²=0.966 |
| $\mu^B$ | f(x) = 65.394 exp( -0.056 x) R²=0.975 | $\sigma^B$ | f(x) = 20.316 exp( -0.019 x) R²=0.975 |
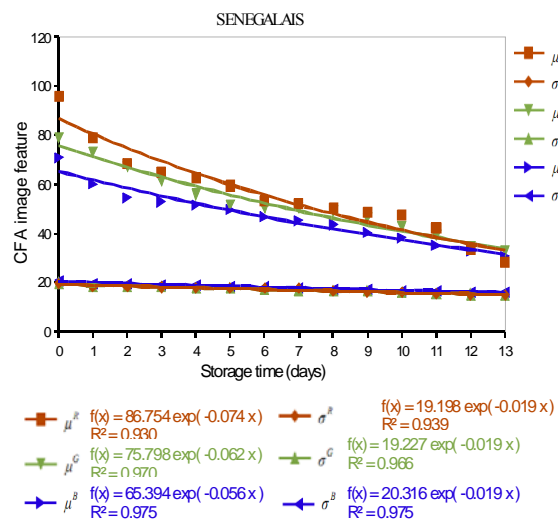
Figure 4c. Relation between 6 CFA image features and storage time in the SENEGALAIS variety

**ECAPAN-021**

$\mu^R$
$\sigma^R$
$\mu^G$
$\sigma^G$
$\mu^B$
$\sigma^B$

CFA image feature — Storage time (days)

| | | | |
|---|---|---|---|
| $\mu^R$ | f(x) = 104.121 exp( -0.043 x) R²=0.978 | $\sigma^R$ | f(x) =32.726 exp( -0.038 x) R²=0.979 |
| $\mu^G$ | f(x) = 76.319 exp( -0.040 x) R²=0.971 | $\sigma^G$ | f(x) =32.847 exp( -0.043 x) R²=0.978 |
| $\mu^B$ | f(x) = 69.538 exp( -0.029 x) R²=0.974 | $\sigma^B$ | f(x) =30.305 exp( -0.039 x) R²=0.870 |
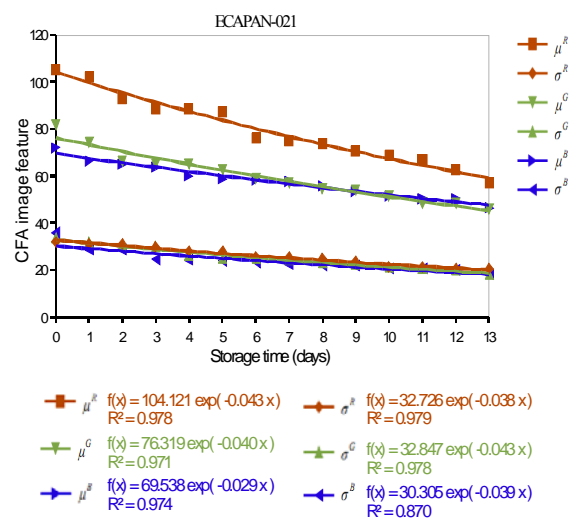
Figure 4d. Relation between 6 CFA image features and storage time in the ECAPAN-021 variety

**MAC-55**

$\mu^R$
$\sigma^R$
$\mu^G$
$\sigma^G$
$\mu^B$
$\sigma^B$

CFA image feature — Storage time (days)

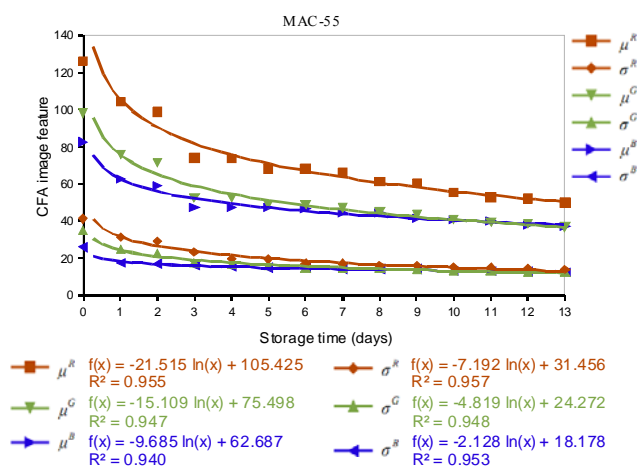| | | | |
|---|---|---|---|
| $\mu^R$ | f(x) = -21.515 ln(x) + 105.425 R² = 0.955 | $\sigma^R$ | f(x) = -7.192 ln(x) + 31.456 R² = 0.957 |
| $\mu^G$ | f(x) = -15.109 ln(x) + 75.498 R² = 0.947 | $\sigma^G$ | f(x) = -4.819 ln(x) + 24.272 R² = 0.948 |
| $\mu^B$ | f(x) = -9.685 ln(x) + 62.687 R² = 0.940 | $\sigma^B$ | f(x) = -2.128 ln(x) + 18.178 R² = 0.953 |

Figure 4e. Relation between 6 CFA image features and storage time in the MAC-55 variety

### 3.3. Multiple linear regression calibration models analysis

For each bean varieties, only the significant CFA image features were used to build a multiple linear regression (MLR) model between the significant features among $\mu^R$, $\mu^G$, $\mu^B$, $\sigma^R$, $\sigma^G$, $\sigma^B$ (as X-variables) and the measured values of the *WAC* (as Y-variables). The calibration set was used to develop the MLR models for predicting the *WAC*. The MLR results for calibration are shown in Table 2. The obtained results show that the behavior of the selected features depends on model of each variety. The feature $\mu^R$ had a positive contribution in all models for *WAC*; being more pronounced in MAC-55 variety. This feature had the similar contribution in the models of DOR-701 and MERINGUE, this mean that the color of DOR-701 and MERINGUE is dominated by redness appearance rather than both greenness and blueness color. Furthermore, $\mu^G$ and $\mu^B$ had an opposite behavior in same model for *WAC*. The $\sigma^G$ feature had the largest contribution in the models for *WAC* of ECAPAN-021 and MAC-55 varieties than the both of the $\sigma^R$ and $\sigma^B$ contributions, this mean that ECAPAN-021 and MERINGUE had both the more dispersion in redness color.

In order to assess the accuracy of the calibration model and to avoid over fitting, calibration parameters were obtained (Table 3). As shown in Table 3, the values of *SEC*, $R^2$and *F* were in the range of 3.65131 to 15.8547, 0.923 to 0.993 and 52.68 to 299.92, respectively. These results show that the values of $R^2$and *F* obtained were in the range for a good calibration model, while the *SEC* values were higher than those recommended by Elmasri*et al*. (2007). The calibration equations presented here is consistent with the finding of Jha*et al.* (2007) using MLR on variables a, b and the product ab (obtained from HunterLab colorimeter) to calibrate for predicting the maturity of mango. However, to verify the generalization ability of calibration models, the present MLR models should be adopted to further investigate the predictive performance for prediction samples.

Table 2.  Form of *WAC* models calibration as a function of CFA image features

| varieties | Models |
|---|---|
| DOR-701 | $\widehat{WAC} = -286.854 + 4.918\mu^R - 0.698\mu^G + 3.663\mu^B$ |
| MERINGUE | $\widehat{WAC} = -33.931 + 4.758\mu^R + 5.338\mu^G - 7.222\mu^B$ |
| SENEGALAIS | $\widehat{WAC} = -81.879 + 1.241\mu^R - 1.692\mu^G + 3.042\mu^B$ |
| ECAPAN-021 | $\widehat{WAC} = -75.64 + 1.415\mu^R + 1.352\mu^G - 3.996\mu^B - 0.766\sigma^R + 7.089\sigma^G + 1.617\sigma^B$ |
| MAC-55 | $\widehat{WAC} = -175.163 + 12.31\mu^R - 23.656\mu^G + 6.297\mu^B + 3.745\sigma^R + 11.795\sigma^G + 0.787\sigma^B$ |

Table 3. Statistical results of MLR models calibration.

| Varieties models | *SEC* | $R^2$ | *F* |
|---|---|---|---|
| DOR-701 | 11.042 | 0.964 | 116.340 |
| MERINGUE | 15.855 | 0.923 | 52.680 |
| SENEGALAIS | 8.227 | 0.948 | 79.670 |
| ECAPAN-021 | 3.651 | 0.993 | 299.920 |
| MAC-55 | 5.609 | 0.959 | 82.610 |

### 3.4. Prediction results for WAC

In order to assess the accuracy of the calibration models and to avoid over fitting, validation values were obtained (Table 4); a calibration model without validation is nonsense. Based on the above results, MLR models were used for measuring *WAC* in prediction samples. Measured values of *WAC* from physico-chemical test (destructive) and its predicted values resulting from MLR models (nondestructive) are shown in Figures 5a–e.

Tables 4 and 3 show that the model was accurate for predicting *WAC* with $R^2$in the range of 0.923 to 0.993 and 0.811 to 0.947 for calibration and validation sets, respectively. The *SEC* and *SEP* were in the range

of 3.651 to 15.855 and 7.587 to 11.669 for calibration and validation sets, respectively. The accuracy of the models in the validation set for predicting *WAC* was with *F* in the range of 52.300 to 221.690. It is obvious for the attribute under study (*WAC*) that the validation tests gave close results as the calibration set indicating good performance of the models for predicting *WAC* nondestructively.

Table 4. Performance of MLR models for predicting *WAC*.

| Varieties models | *SEP* | bias | $R^2$ | *F* |
|---|---|---|---|---|
| DOR-701 | 11.669 | -0.224 | 0.878 | 87.060 |
| MERINGUE | 11.378 | 4.010 | 0.811 | 52.300 |
| SENEGALAIS | 10.834 | 8.397 | 0.879 | 87.680 |
| ECAPAN-021 | 7.587 | 4.713 | 0.947 | 221.690 |
| MAC-55 | 8.816 | 1.168 | 0.912 | 197.450 |
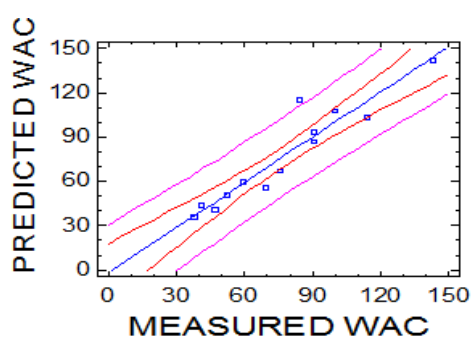


Figure 5a. The prediction results for WAC of DOR-701 variety by using MLR model, resulting in SEP = 11.669, $R^2$ = 0.878 and F = 87.060
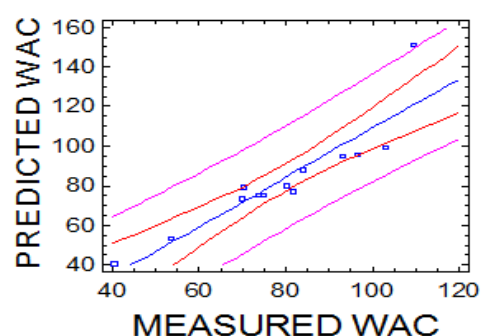


Figure 5b. The prediction results for WAC of MERINGUE variety by using MLR model, resulting in SEP = 11.378, $R^2$ = 0.811 and F = 52.300
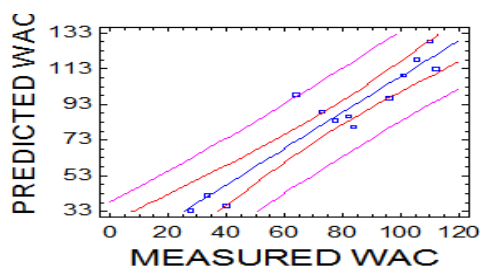


Figure 5c. The prediction results for WAC of SENEGALAIS variety by using MLR model, resulting in SEP = 10.834, $R^2$ = 0.879 and F = 87.680
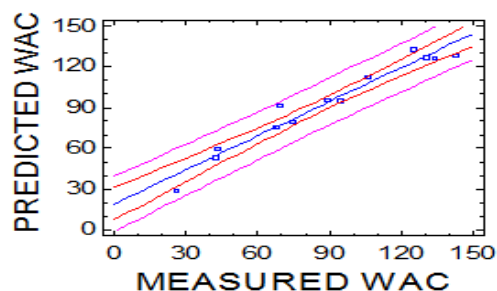


Figure 5d. The prediction results for WAC of ECAPAN-021 variety by using MLR model, resulting in SEP = 7.587, $R^2$ = 0.947 and F = 221.690
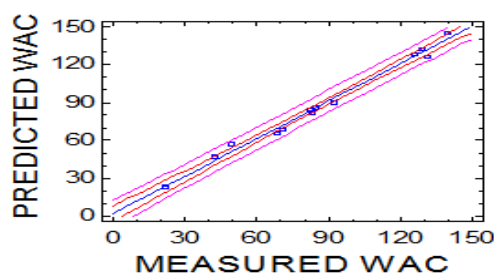


Figure 5e. The prediction results for WAC of MAC-55 variety by using MLR model, resulting in SEP = 8.816, $R^2$ = 0.912 and F = 197.450.

## 4.    CONCLUSION

Storage of these five bean varieties under adverse conditions of high temperature and relative humidity rendered them susceptible to the hardening phenomenon. Several changes in grain quality characteristics were affected by storage under these adverse conditions: loss of color lightness and development of browning and darkening ; and decrease in *WAC*. For practical and low cost application, *WAC* of beans was predicted from CFA image features. By multiple linear regression (MLR), precise calibration equations were obtained. The calibration models were validated successfully. The results show that the nondestructive determination of *WAC* of common beans using CFA image features is reliably possible. It is also known that the established models is low cost and high precision, but less robust due to the higher values of *SEC* and *SEP*. In the future, more work will be done to optimize and implement this technique by using other algorithms, such as neural networks, wavelet transform and genetic algorithm, for many other bean grain varieties that differ by season or growing region.

## REFERENCES

[1]  Reyes-Moreno C, Okamura-Esparza J, Armienta-Rodelo E, Gomez-Garza RM, Milan-Carrillo J. Hard-to-cook phenomenon in chickpeas (cicerarietinum L): Effect of accelerated storage on quality. *Plant Foods for HumanNutrition* 2099; 55: 229–241.

[2]  De Almeid Costa GE, Da Silva Queiroz-Monici K, Machado Reis SMP, De Oliveira AC. Chemical composition, dietary fiber and resistant starch contents of raw and cooked pea, common bean, chickpea and lentil legumes. *Food Chemistry*. 2006; 94: 327–330.

[3]  Mariana Marques Correa, Lucia M Jaeger de Carvalho, Marilia ReginiNutti, Jose Luiz Viana de Carvalho, Antonio R HohnNeto, Ediane M Gomes Ribeiro. Water absorption,hard shell and cooking time of common beans (*Phaseolus vulgaris L.*).*African Journal of Food Science andTechnology*. 2010; 1(1): 013–020.

[4]  Jood S, Mehta U, Singh R. Effect of processing on available carbohydrates in legumes. *Journal of Agriculture and Food Chemistry*. 1986; 34(3); 417–420.

[5]  De-León L, Elias LG, Bressai R. Effect of salt solutions on the cooking time, nutritional and sensory characteristic of common beans.*Food Research International*. 1992; 25(2): 131–136.

[6]  Barampama Z, Simard R. Oligosaccharides, antinutritional factors, and protein digestibility of dry beans as affected by processing.*Journal of Food Science*. 1994; 59(4): 833–838.

[7]  Varriano-Marston E, Jackson GM. Hard-to-cook phenomenon in beans : Structural changes during storage and inhibition. *Journal of Food Science*. 1981; 46(5): 1379–1385.

[8]  Hincks MJ, Stanley DW. Multiple mechanisms of beans hardening. *Journal of Food Technology*. 1986; 21: 731–750.

[9]  Hentges D, Weaver C, Nielsen S. Reversibility of the hard-to-cook defect in dry beans (*Phaseolus vulgaris*) and cowpeas (*Vignaunguiculata*).n*Journal of Food Science*. 1990; 55: 1474–1476.

[10] Hentges D, Weaver C, Nielsen S. Changes of selected physical and chemical components on the development of the hard-to-cook bean defect. *Journal of Food Science*. 1991; 56: 436–442.

[11] Nyakuni G, Kikafunda J, Muyonga J, Kyamuhangire W, Nakimbugwe D, Ugen M. Chemical and nutritional changes associated with the development of the hard-to-cook defect in common beans. *International Journalof Food Sciences and Nutrition*. 2008; 59: 652–659.

[12] Giselle A Maurer, Banu F Ozen, Lisa J Mauer, Suzanne S Nielsen. Analysis of Hard-to-Cook red and black common beans using Fourier Transform Infrared Spectroscopy. *Journal of Agricultural and Food Chemistry*. 2004; 52: 1470–1477.

[13] Hentges DL, Weaver CM, Nielson SS, Weaver LR, Evans BH, Jacob JM. Automation of a mattson bean cooker for testing the hard-to-cookdefect in legume seeds. *Transactions of the ASAE (American Society of Agricultural Engineers)*. 1990; 33(2): 625–628.

[14] Ning Wang, James K Daun. Determination of cooking times of pulses using an automated mattson cooker apparatus. *Journal of the Science of Food and Agriculture*. 2005; 85(18): 1631–1635.

[15] Bitjoka L, Teguia JB, Mbofung CMF. PC-based instrumentation system for the study of bean cooking kinetic. *Journal of Applied Sciences*. 2008; 8(6): 1103–1107.

[16] Bitjoka L, BoukarOusman, TeninDzudie, Mbofung CMF, Tonye E. Digital camera images processing of hard-to-cook beans. *Journal of Engineering andTechnology Research. 2010;* 2(9): 177–188.

[17] Del Moral FG, O'Valle F, Masseroli M, Del Moral RG. Image analysis application for automatic quantification of intramuscular connective tissue in meat. *Journal of FoodEngineering*. 2003; 81: 33–41.

[18] Fernando Mendoza, Petr Dejmek, José M Aguilera. Calibrated color measurements of agricultural foods using image analysis. *Postharvest Biology and Technology*. 2006; 41: 285–295.

[19] Otsu A. A threshold selection method from gray-level histograms. *IEEE Transactions on Systems, Man and Cybernetics*. 1979; 15: 652–655.

[20] Chaoxin Zheng Da-Wen Sun, Liyun Zheng. Correlating colour to moisture content of large cooked beef joints by computer vision. *Journal of Food Engineering*. 2006; 77: 858–863.

[21] Gamal ElMasry, Ning Wang, Adel ElSayed, Michael Ngadi. Hyperspectral imaging for nondestructive determination of some quality attributes for strawberry. *Journal of Food Engineering*. 2006; 81: 98–107.

[22] Jha SN, Sangeeta Chopra, Kingsly ARP. Modeling of color values for nondestructive evaluation of maturity of mango. *Journal of Food Engineering*. 2007; 78: 22–26.

[23] Yande Liu, Xingmiao Chen, AiguoOuyang. Non destructive determination of pear internal quality in dices by visible and near-infrared spectrometry. *LWT – Food Science and Technology*. 2008; 41: 1720–1725.

[24] Bart M Nicolaï, KatrienBeullens, ElsBobelyn, Ann Peirs, WouterSaeys, Karen I Theron, JeroenLammertyn. Non destructive measurement of fruit and vegetable quality by means of NIR spectroscopy: a review. *Postharvest Biology and Technology*. 2007; 46: 99–118.

[25] De-León LF, Bressani R, Elías LG. Effect of seed coat on the hard-to-cook phenomenon of common beans (*Phaseolus vulgaris*). *Archives Latinoamericaines de Nutrition*. 1989; 39: 405–407.

[26] Deshpande SS, Cheryan M. Microstructure and water uptake of  Phaseolus and winged beans. *Journal of Food Science*. 1986; 51: 1218–1223.

[27] Ngatchou A, Bitjoka L, BoukarOusman Tonye E. Color and Texture Information Processing to Improve Storage Beans.*British  Journal of Applied Science and Technology.* 2012; 2(2): 96–111.

## BIOGRAPHIES OF AUTHORS

Ousman Boukarreceived the B.A., M.A.,degrees from the University of Ngaoundere, Cameroon. His main research interests are food images analysis, automation production systems, and food nondestructive testing.



Laurent Bitjoka is an Associate Professor at the National Advanced School of Agro-Industrial Sciences. His main research interests are signal processing, images processing and Biosystem.



GamraïkréoDjaowéreceived the B.A., M.A.,degrees from the University of Ngaoundere, Cameroon. He is a technical researcher at the Faculty of Science of the University of Ngaoundere.His main research interests are food images analysis, electrical engineering, and food nondestructive testing.